Keywords: ammonia combustion concepts, ammonia high-pressure direct injection

High-pressure ammonia-diesel dual fuel combustion in medium-speed engines

Prof. Nicole Wermuth[1,2], Dr. Maximilian Malin[1], Markus Roßmann[1], Prof. Andreas Wimmer[1,2], Dr. Marco Coppo[3]

(1) LEC GmbH – Large Engines Competence Center, (2) Graz University of Technology, (3) Officine Meccaniche Torino SpA

https://doi.org/10.18453/rosdok_id00004640

Abstract

Ammonia combustion in internal combustion engines has been the focus in many research projects in recent years. One of the drawbacks of many applications with gaseous ammonia admission is the high level of pollutant emissions, nitric oxide and unburned ammonia in particular. The use of high-pressure liquid ammonia injection has the potential to reduce the level of these harmful emissions. This article presents the application of a fuel-actuated common rail injector prototype developed by OMT in a large-bore medium speed single cylinder research engine at the LEC GmbH. Building on initial insights from the fuel spray characterization in an optically accessible constant volume chamber, the injector was integrated into a cylinder head in a dual-fuel configuration with a diesel pilot injector. The focus of the test campaign was the investigation of different fuel injection strategies and operating parameters and their impact on engine combustion performance and emissions. The combustion concept allowed operation with an ammonia fuel fraction up to 90% and showed robust operation even at moderate injection pressures of around 60 MPa. A wide operating window with regard to excess air ratio and combustion phasing could be achieved and will be the foundation for further load increases and performance improvements.

1. Introduction

The global carbon dioxide (CO_2) concentration in the atmosphere has already passed the 420-ppm mark in the last couple of years [1]. According to the Copernicus Climate Change Service global temperatures reached exceptionally high levels in 2023, making it the warmest year on record – overtaking by a large margin 2016, the previous warmest year [2].

In order to limit global warming to 1.5 K above pre-industrial levels [3], a goal that was agreed on at the UN Climate Change Conference [4] the emission of CO_2 and other gases with a high global warming potential (GWP) must be reduced quickly. Governments worldwide put forward ever more ambitious greenhouse gas (GHG) emission reduction targets. The 2030 Climate Target Plan of the European Commission sets the European Union on a path to becoming climate neutral by 2050 and proposed to reduce GHG emissions at least by 55% of the 1990 levels by 2030 [5]. In February 2024 the European Commission deemed it necessary to accelerate the previous plans and recommended a 90% net GHG emission reduction by 2040 [6] as illustrated in Figure 1. The International Maritime Organization (IMO) first established targets to reduce CO_2 emissions in 2018 [7] and set even more ambitious goals in 2023 to achieve net-zero GHG emissions by 2050, with indicative intermediate points of 40% CO_2 reduction per transport work in 2030 and a total GHG emission reduction of 70% by 2040 compared to 2008.

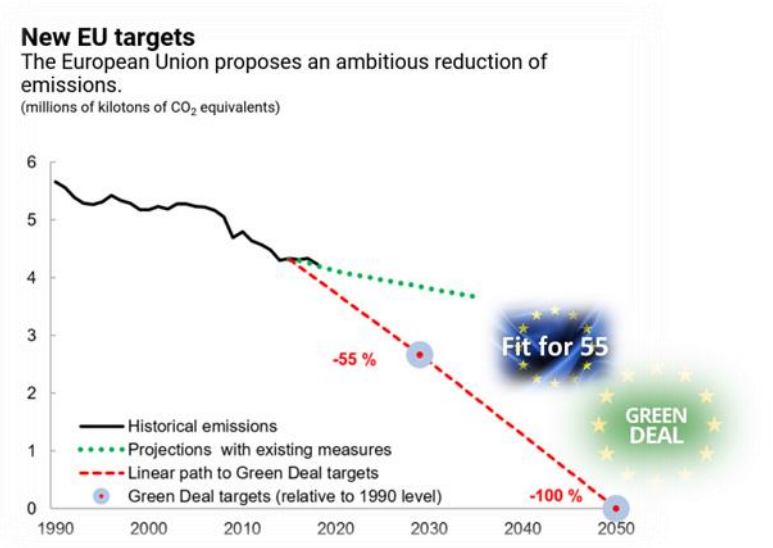

Figure 1: European Union targets for greenhouse gas emission reduction

Achieving these ambitious goals requires a global transition from fossil fuels to renewable energy sources. The volatility of these sources and the fact their production and their consumption will to a large extent take place in different regions of the world will make it necessary to store and transport energy on a large scale. Storage in the form of chemicals offers large storage capacities over long periods of time and even seasonal storage (Figure 2).

These secondary energy carriers can be used as e-fuels to decarbonize transportation, such as aviation, shipping and heavy duty on- and off-road applications. DNV GL's scenario for the path to net-zero emissions [9] shows a diverse future energy mix for the maritime sector and projects ammonia (NH_3) to be the dominant fuel in the maritime sector by 2050. The projected use of ammonia as a hydrogen

carrier and as a fuel in maritime transport and power generation is expected to drive a three to four-fold increase of global ammonia consumption by 2050. As of 2024 several engine OEMs already announced future product offerings.

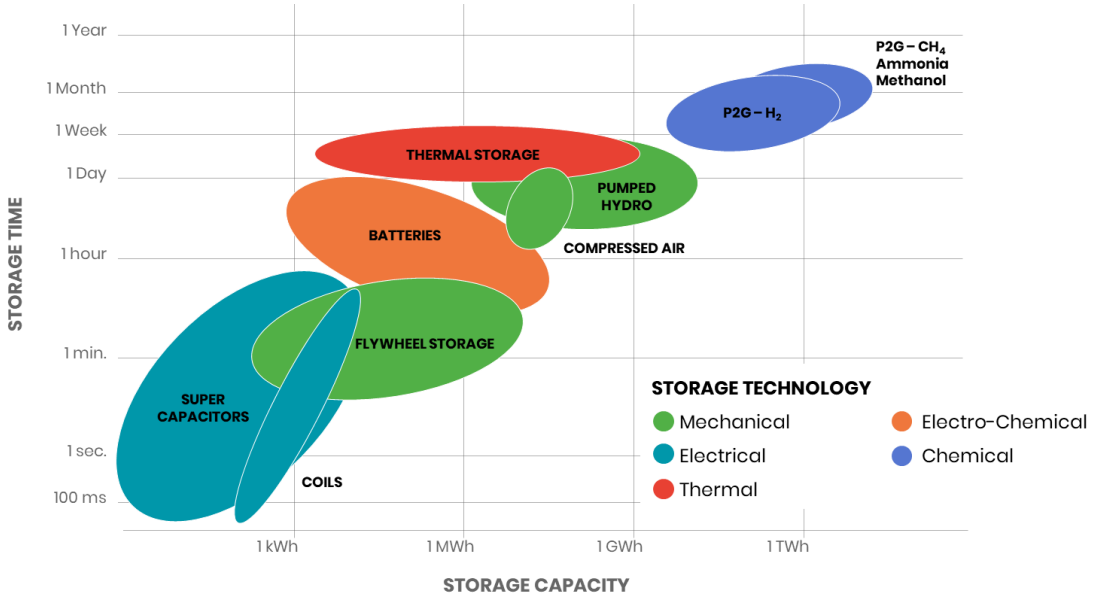

Figure 2: Energy storage options [8]

This article presents experimental results of research work on the use of liquefied high-pressure ammonia injection in a combustion concept for medium-speed large-bore compression ignition engines. The focus of study was the impact of engine operating parameters on the engine performance and exhaust gas emissions. Based on the properties of ammonia, the advantages and challenges for engine combustion systems are discussed. The selected combustion system and the operating procedures are described and experimental measurement results are presented. Finally, a comparison of the most important parameters with a diesel combustion system is shown and further possibilities for improvement are discussed.

2. Ammonia engine combustion concepts

The physical and chemical properties of ammonia differ significantly from those of fossil fuels typically used in large-engine applications and also from those of other e-fuels. Table 1 provides an overview of properties for several carbon-based and carbon-free fuels relevant for large-engine applications. Especially the low laminar flame speed and the high minimum ignition energy of ammonia in comparison to other e-fuel options are often considered to be detrimental for use in an internal combustion engine.

To overcome the challenges posed by the ammonia ignition and combustion properties, admixing of a more reactive fuel was proposed [10]. For marine applications where redundancy requirements are usually adhered to by providing diesel engine operation capability, diesel fuel is used in ongoing research as the reactive fuel component. For spark ignition applications hydrogen is a suitable high reactivity fuel.

Table 1: Fuel properties of selected e-fuels

Fuel	Lower heating value (gravimetric) [MJ/kg]	Lower heating value (volumetric) [MJ/kg]	Laminar flame speed (stoichiometric) [m/s]	Min. ignition energy [mJ]	Autoignition temperature [K]
Drop-in e-fuel (diesel-like)	43	36	0.87	0.23	483
e-methane	50	36	0.38	0.29	868
e-methanol	19	15	0.36	0.14	712
e-ammonia (liquid, - 33 °C)	20	14	0.07	8.000	930
e-hydrogen (liquid, - 253 °C)	120	9	3.50	0.017	858

There a various fuel admission and ignition concept that are feasible for ammonia-fueled engines. An overview of currently considered concepts is shown schematically in Figure 3.

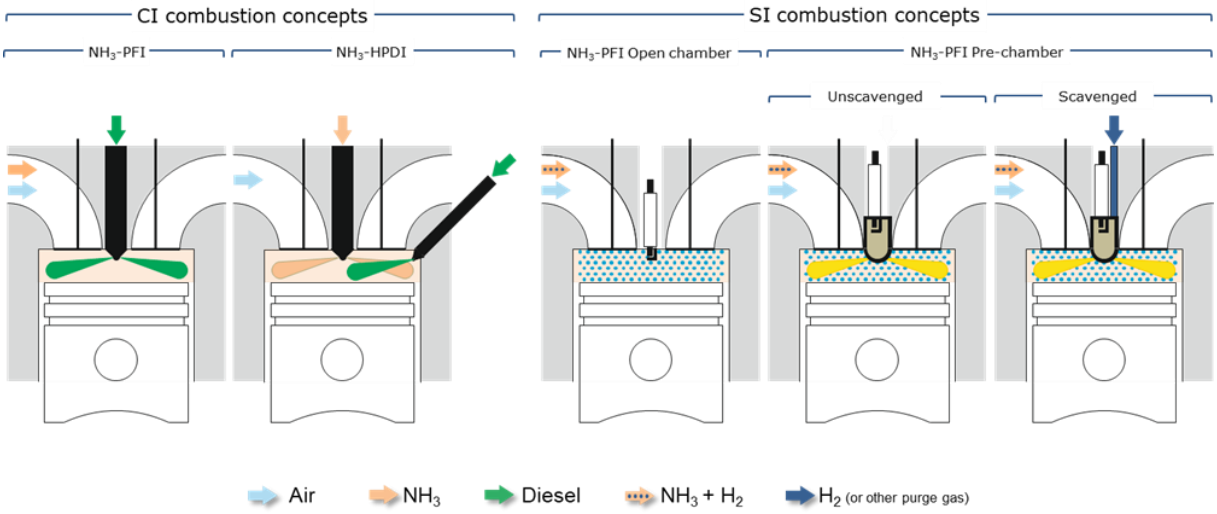

Figure 3: Compression ignition and spark ignition combustion concepts

Spark ignition (SI) concepts span the range from direct ignition concepts with a centrally mounted spark plug in the main combustion chamber (NH_3-PFI Open chamber) to pre-chamber ignition concepts with different scavenging variants (NH_3-PFI Pre-chamber). The pre-chamber concept enables mixture stratification with a fuel-rich mixture in the pre-chamber or additional hydrogen supply directly into the pre-chamber to enhance the ignition conditions at the spark plug location. These engine concepts predominantly use external mixture formation of gaseous ammonia and air either upstream of the turbocharger or via port fuel injection.

Ammonia compression ignition (CI) concepts are typically designed as dual fuel combustion concepts with diesel pilot injection. Gaseous low-pressure ammonia admission (NH_3-PFI) can be realized with

either central mixing of ammonia with air upstream of the turbocharger or the introduction of ammonia via port fuel injection. Diesel is injected directly into the combustion chamber at the end of the compression stroke to initiate the combustion process which relies on flame propagation in the ammonia-air mixture. The combustion process of liquid high-pressure ammonia injection (NH_3-HPDI) is similar to typical diesel combustion where the combustion is controlled by fuel-air mixing. This concept uses either two fuel injectors in the combustion chamber or a two-needle injector.

The pollutant emission formation of ammonia combustion is dominated by the fuel-bound nitrogen and often associated with the emission of nitrous oxide (N_2O) which, according to the IPCC has a GWP 273 times that of CO_2 for a 100-year timescale [11].

The authors previously investigated combustion concepts using gaseous ammonia admission via port fuel injection or central mixture formation in four-stroke engines [12, 13]. In those experiments considerable concentrations of unburned ammonia in the order of 5000 ppm were measured in the exhaust gases. One mitigation measure was a reduction of the excess air ratio compared to diesel or natural gas engine operation. Ammonia spray combustion has the potential to reduce the ammonia emissions and nitrogen oxide (NO_X) formation while also maintaining a high excess air ratio.

3. Experimental test set-up

3.1. Single cylinder research engine

The engine investigations were carried out on a medium-speed 4-stroke single cylinder research engine (SCE) with a displacement volume of approximately 15 liters that was modified for dual fuel operation. For the investigation of the diesel-ammonia operation, a non-reentrant piston bowl and a compression ratio (CR) of 17:1 were chosen.

The low-swirl cylinder head was equipped with two intake and two exhaust valves. Exchanging the cam shaft lobes allowed a modification of the valve lift curves. Additionally, the valve timing could be adjusted individually for the intake and the exhaust valves. For this investigation, an intake valve lift profile with early intake valve closing (IVC) before bottom dead center was selected. The engine configuration is summarized in Table 2.

Table 2: Engine specification

Parameter	**Value**
Rated speed	750 rpm
Bore	250 mm
Stroke	320 mm
Compression ratio	17:1
Valve timing	Early IVC
No. of intake/exhaust valves	2/2
Charge air	Provided by external compressors with up to 1 MPa boost pressure

The cylinder head used on the single cylinder research engine was based on the serial configuration but was modified for the dual fuel operation. The ammonia injector was located centrally in the combustion chamber, replacing a conventional diesel injector, and a second injector was integrated into the cylinder head to deliver the diesel pilot injection.

The design of the cylinder head did not allow for a vertical positioning of the diesel pilot injector but rather a lateral, inclined positioning was required. The positioning and orientation of the diesel injector nozzle in the combustion chamber required a special spray hole configuration. An illustration of the fuel jet interaction of the diesel spray and the ammonia spray is shown in Figure 4.

Additionally, the cylinder head was modified to provide two separate fuel return passages from the ammonia injector. While one of the fuel return streams was maintained at atmospheric pressure, the second stream was maintained at 5 MPa to avoid two-phase flow conditions in the injector control valve.

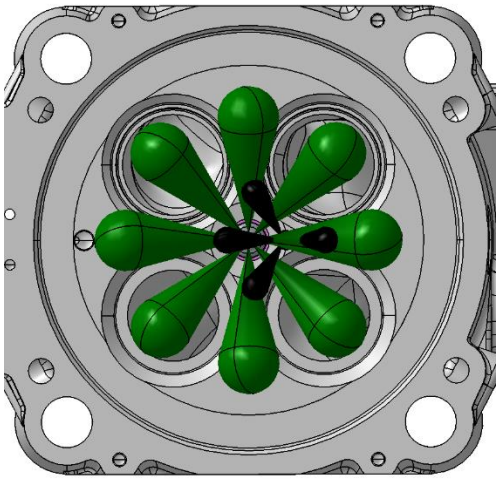

Figure 4: Illustration of diesel pilot (black) and ammonia (green) fuel jet interaction

The injector basic architecture was chosen to be a common rail (CR) arrangement, with a two-way, solenoid actuated control valve cooperating with two calibrated orifices to modulate pressure in a control chamber realized on top of the nozzle needle to actuate its opening and closing motion, an

integrated fuel accumulator and flow limiter valve, and a nozzle with zero static leakage, as described in [14] and [15].

All engine fluids including cooling water, lubricating oil, and charge air were controlled to ensure well-defined and reproducible testing conditions. Instead of a turbocharger, an air compressor upstream of the engine and a flap in the engine exhaust system were used to adjust intake and exhaust manifold pressures. A flush mounted piezoelectric cylinder pressure transducer enabled real-time calculation of the indicated mean effective pressure of each cycle.

The excess air ratio (EAR) is defined in Equation 1 and is taking the mass of ammonia m_{NH3}, the mass of diesel m_{diesel} and the mass of air m_{air} as well as the stoichiometric air-fuel ratios of ammonia $AFR_{stoich,NH3}$ and diesel $AFR_{stoich,diesel}$ into account.

$$EAR = \frac{m_{air}}{m_{NH_3} * AFR_{stoich,NH_3} + m_{diesel} * AFR_{stoich,diesel}} \quad (1)$$

In order to acquire highly reliable and reproducible exhaust gas measurements, an FTIR system was used to cover the whole range of exhaust gas components of interest. Table 3 summarizes the SCE measurement instrumentation.

Table 3: Overview engine instrumentation

Quantity	Instrumentation	Accuracy	Range
Air mass flow	Emerson Micro Motion CMF100	+/-0.35%	0 – 300 kg/h
Diesel mass flow	AVL Fuel Exact MF 150KG SF	+/-0.1%	0 – 150 kg/h
Ammonia mass flow	Emerson Micro Motion CMFS025	+/-0.1%	10 – 180 kg/h
Charge air temperature	PT 100	+/- 0.15 K * 0.002 * (t)	223 – 773 K
Charge air pressure	AVL piezoelectric transducer GU21C	+/-0.3%	0 – 8 MPa
Cylinder pressure	AVL piezoelectric transducer QC34C	+/-0.2%	0 – 25 MPa
Exhaust gas temperature	Thermocouple type K	0.004 * (t)	max. 1370 K
Exhaust gas pressure	AVL piezoelectric transducer GU21C	+/-0.3%	0 – 8 MPa

3.2. High-pressure fuel injection systems

A dedicated ammonia high-pressure fuel supply and injection systems was built for the test campaign. The main challenges in designing the system were to avoid ammonia evaporation under all operating conditions and to fulfill minimum inlet pressure requirements of the high-pressure fuel pump.

Table 4: Fuel injection equipment

Component	**Specification**
Diesel pump	Bosch
Diesel pilot injector	DUAP
Diesel pilot nozzle configuration (holes / flow rate / reference pressure)	4-hole, 1.6 l/min, 120 MPa
Ammonia fuel pump	Hammelmann HAMPRO 23
Ammonia injector	OMT common rail injector
Ammonia nozzle configuration (drilling / flow rate / reference pressure)	8 x 0.54 mm, 14 l/min, 131 MPa

Two independent high-pressure fuel systems were built for the diesel pilot and the ammonia injection. The diesel pilot injection system was capable of operating up to 120 MPa, and the pilot nozzle used had a nominal flow rate of 1.6 l/min. The pilot fuel flow rate was measured via an AVL Fuel Exact. The ammonia injector was equipped with an 8-hole nozzle with a nominal flow rate of 14 l/min. The nozzle was designed for 131 MPa and the maximum operation pressure of the injector was set at 150 MPa. The fuel injection equipment specification is summarized in Table 4.

The high-pressure fuel system for ammonia included a pump designed for a maximum injection pressure of 150 MPa. The high-pressure fuel system also included the fuel conditioning, the fuel mass flow rate measurement and the actuators and controls to maintain the desired pressure in the injector leakage return line. A schematic of the ammonia high-pressure system is depicted in Figure 5.

In addition to the dual-fuel combustion concept the SCE could also be equipped with a centrally mounted diesel injector to allow pure diesel operation. The diesel engine operation was tested with a different injector and nozzle set-up that resembled the serial production configuration.

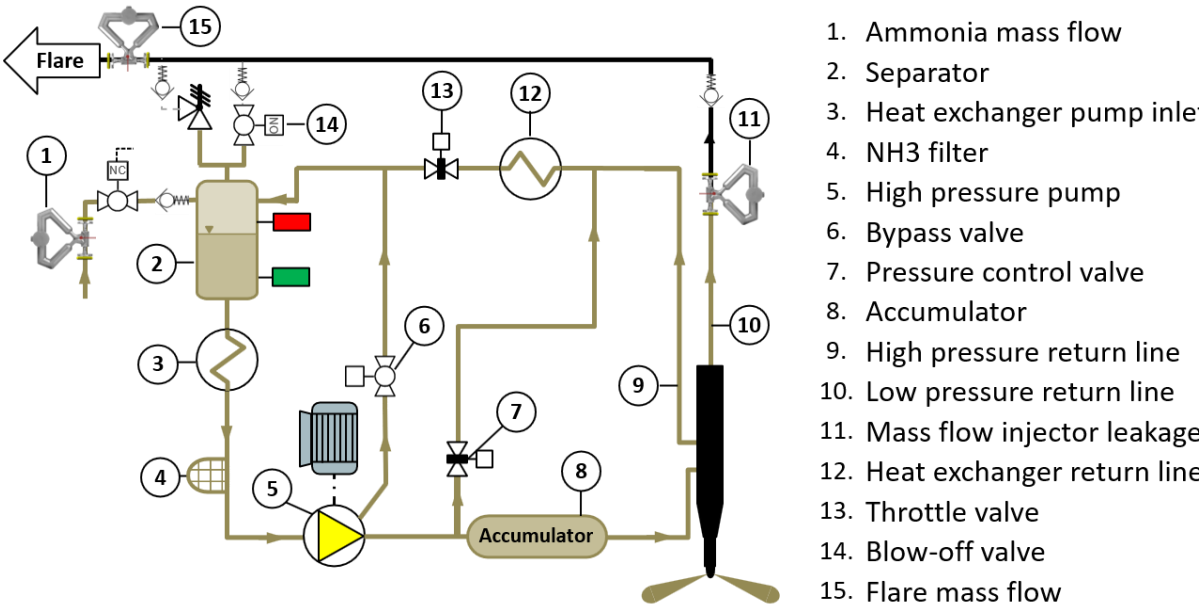

Figure 5: Ammonia high-pressure supply system

4. Experimental investigations

4.1. Test procedures

The goal of the experimental investigations with ammonia direct injection was to assess the impact of fuel injection strategies and operating parameters such as excess air ratio and combustion phasing. During the SCE investigations the key operating parameters, e.g. excess air ratio, diesel fraction, injection timing, were varied for a fixed load of 1.2 MPa brake mean effective pressure (BMEP) at a constant engine speed of 750 rpm. The excess air ratio was determined from the measured air and fuel mass flow rates and the stoichiometric air-to-fuel mass ratio for the selected share of diesel and ammonia fuel. Adjustment of the excess air ratio was achieved via boost pressure adjustment. Exhaust gas pressure was adjusted to achieve a desired ratio of boost pressure to exhaust gas pressure.

The dual fuel combustion concept with separate injectors for diesel and ammonia allows an independent adjustment of the dwell between the injection of the two fuels. Figure 6 illustrates the definition of the dwell which describes the crank angle duration from the start of the diesel injector current signal to the start of the ammonia injector current signal. Due to the hydraulic delay the injection starts later than the injector current signal which is indicated by the rail pressure drop (shown for ammonia in Figure 6). The hydraulic delay of the diesel injector amounts to only a few degrees crank angle while the ammonia injector hydraulic delay is longer (around ten degrees crank angle) and varies with the rail pressure. Since the detection of the start of injection is subject to a higher uncertainty than the injector current signal, the dwell timing will be calculated based on the injector current signals throughout the article.

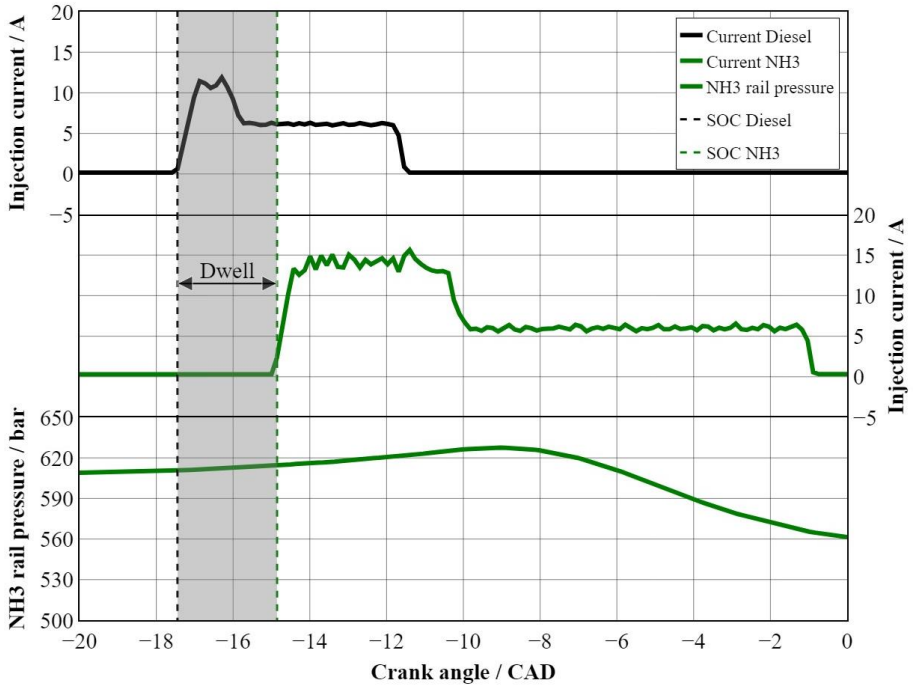

Figure 5: Definition of dwell, injector current signals and ammonia rail pressure trace

4.2. Excess air ratio variation

An excess air ratio variation between 1.2 and 1.8 was performed at a fixed combustion phasing – defined as the crank angle where 50% of the fuel energy has been released (CA50). Both the ammonia and the diesel rail pressures were maintained at a constant value of 60 MPa and 120 MPa, respectively. The diesel energetic fraction was maintained at 10% and the dwell duration was fixed at 2.5 degree crank angle (CAD) throughout the test. The injection timing that is required to achieve the desired combustion phasing is shown on the bottom of Figure 7. Towards lower excess air ratios, the start of the injector energization (start of current – SOC) had to be advanced by approximately 1 CAD which is mainly driven by a longer ignition delay time and the early part of the combustion process. The time when 5% of the fuel energy has been released (CA05) is nearly constant for the whole excess air ratio variation. A larger variation can be observed in the timing of 90% heat release (CA90). While there is only a small change between EAR = 1.8 and 1.4 there is an observable shift to later timings of CA90 for the lowest EAR = 1.2.

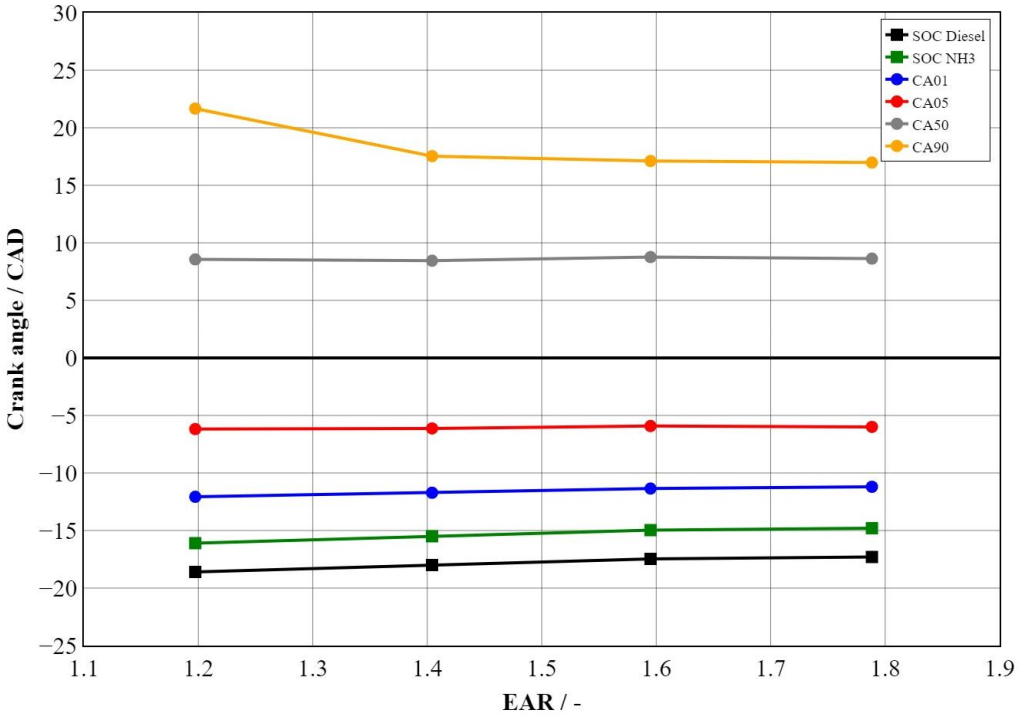

Figure 6: Injection timing and combustion progress for an EAR variation at constant BMEP

The impact of the excess air ratio on the combustion process is depicted in Figure 8 and Figure 9. In the upper part of both figures the injection timings for both the ammonia and the diesel injection are displayed. The small difference in the lengths of the injections for different excess air ratios is reflecting the efficiency benefit of the higher excess air ratios. In Figure 8 the normalized heat release rates for the early combustion phase are shown. It can be observed that the time delay between the start of the diesel injection and the first rise of the heat release rate decreases with increasing excess air ratio. Due to the long hydraulic delay of the ammonia injector the ammonia injection started only after the first heat release was observed and it is assumed that the variance in ignition delay is caused by oxygen availability. Similar to the behavior that is familiar from diesel combustion processes the fuel-air mixture that is formed within the ignition delay time is burned rapidly when the combustion starts, resulting in the well-known pre-mixed peak in the heat release rate. It is assumed that no ammonia is present in the combustion chamber at this point in time and the small differences in the height of the pre-mixed peaks are the result of different ignition delay times.

Figure 9 depicts the cumulative heat release for the same four operating conditions. Up to approximately 80% of total heat release the combustion process is nearly identical for all excess air ratios. Beyond this point the combustion proceeds considerably faster with higher excess air ratios, likely determined by the local availability of oxygen.

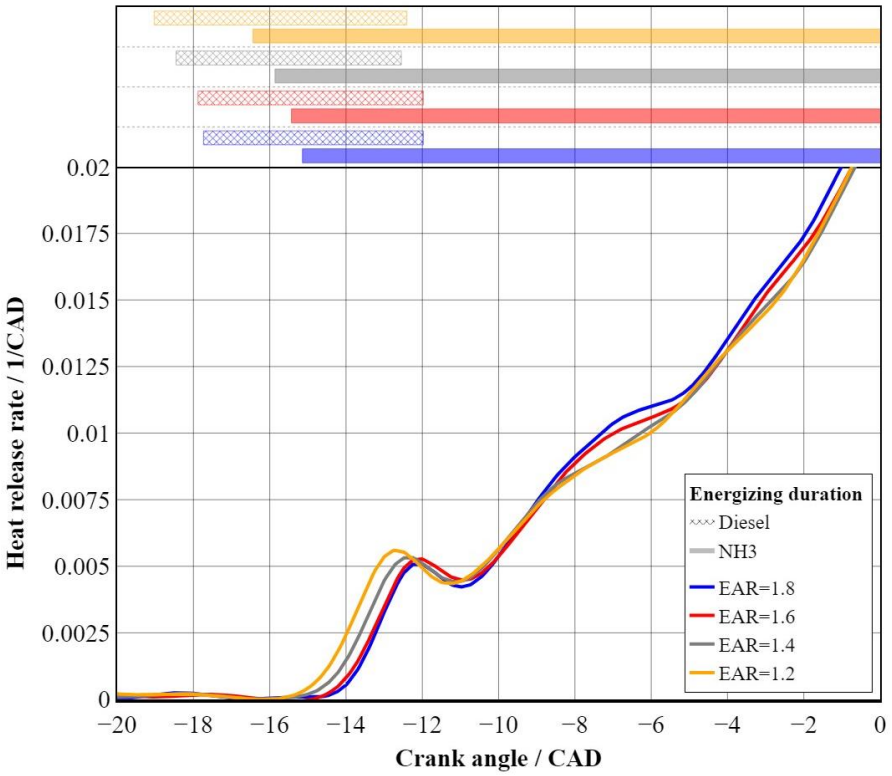

Figure 7: Heat release rate during ignition and early combustion phase for different EAR at constant BMEP

The process for the lower excess air ratio is not just characterized by a delayed heat release but also by a less complete combustion as can be seen in the emissions of unburned ammonia that are displayed in the top graph of Figure 10.

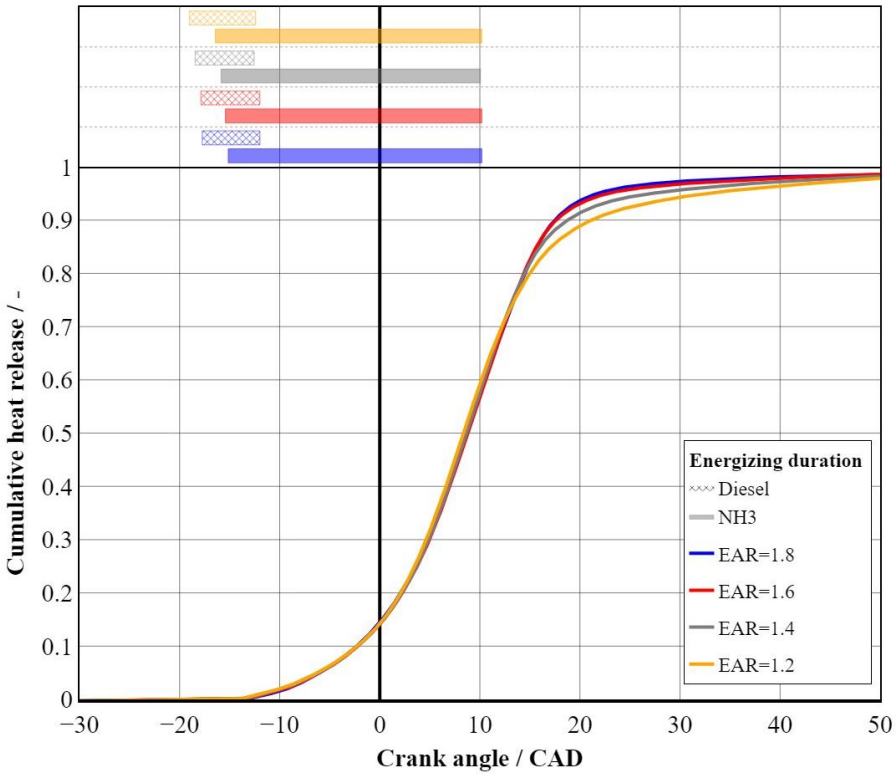

Figure 8: Cumulative heat release for different EAR at constant BMEP.

While the measured NH_3 concentrations in the exhaust gas are nearly constant between EAR = 1.4 and 1.8 there is a significant increase for EAR = 1.2. The opposite is observed for the emissions of nitrogen oxides that are lower for EAR =1.2 than for the higher excess air ratios. While the retarded and less complete combustion might contribute to this behavior, oxygen availability is likely the dominating factor. This is in line with the trends reported in the literature for (partially) premixed combustion where maximum nitrogen oxide emissions were found to occur at approximately EAR = 1.35 [16]. Taking the changing efficiency and exhaust gas mass flow rates for different excess air ratios into account the NO_X emission intensity for EAR = 1.2 was found to be approximately 40% of that for the higher excess air ratios shown in Figure 10.

The nitrous oxide emissions are on a relatively low level below 50 ppm. Due to the high global warming potential of nitrous oxide a further reduction via exhaust gas aftertreatment is still required to achieve the zero-impact emission levels. The nitrous oxide concentrations are decreasing with decreasing excess air ratio from 1.8 – to 1.4 as was found in experiments with homogeneous ammonia-air mixtures [12, 13]. For EAR = 1.2 an unexpected increase of the nitrous oxide emissions was observed. Since this increase is occurring in conjunction with a strong increase of the ammonia concentration it is possible that the nitrous oxide (or at least some share) is not formed during the main combustion phase but rather in the expansion and exhaust stroke when the unburned ammonia is reacting with nitrogen oxides at low temperature in a reaction known as selective non-catalytic reduction [17].

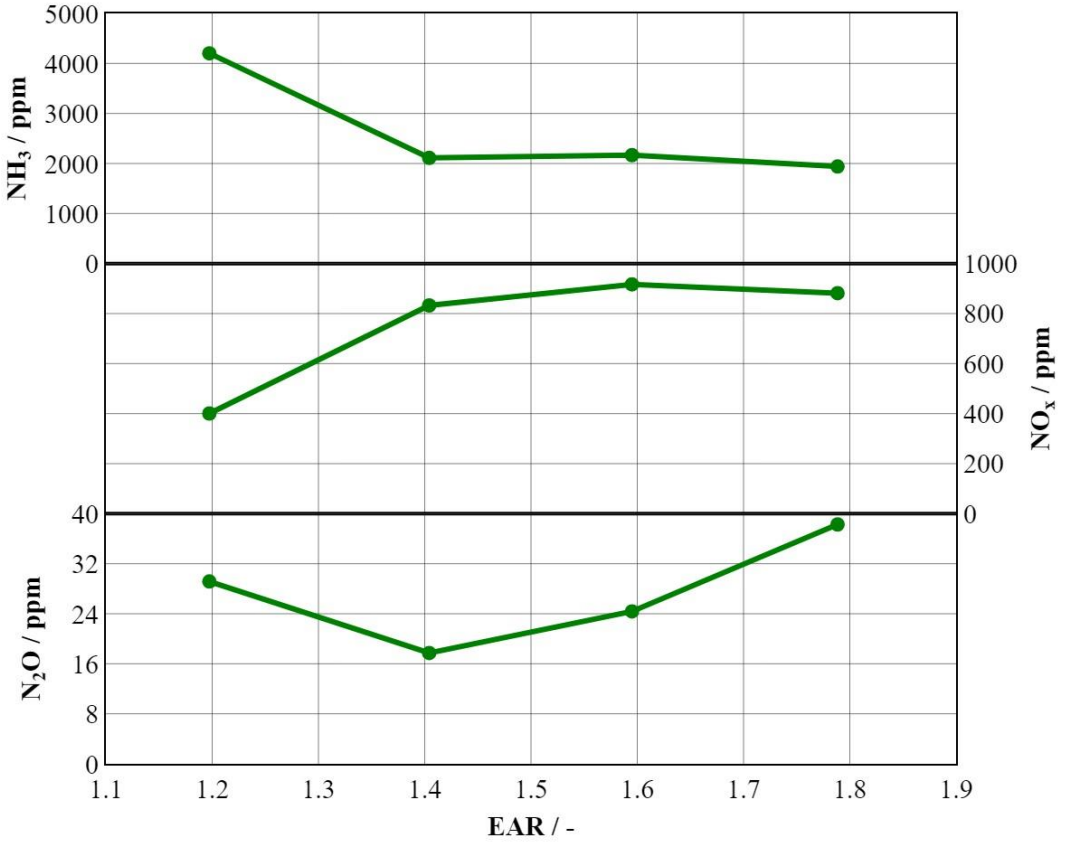

Figure 9: NH_3, NO_X and N_2O emission concentrations for an EAR variation at constant BMEP

The results show that the excess air ratio for ammonia-diesel dual fuel operation can be varied in a wide range and that an excess air ratio similar to values for typical diesel engines is feasible.

4.3. Combustion phasing variation

A combustion phasing variation between CA50 = 4 CAD after top dead center (aTDC) and 16 CAD aTDC was performed for an excess air ratio of 1.8. Both the ammonia and the diesel rail pressures were maintained at a constant value of 60 MPa and 120 MPa, respectively. The diesel energetic fraction was maintained at 10% and the dwell duration was fixed at 2.5 CAD throughout the test. The injection timing that is required to achieve the desired combustion phasing is shown on the bottom of Figure 11. In contrast to what would be expected, i.e., disproportionally advanced injection timing to achieve the earlier combustion phasing due to the increasing ignition delay time, it was observed that the injection timing had to be advanced less than the respective target combustion phasing.

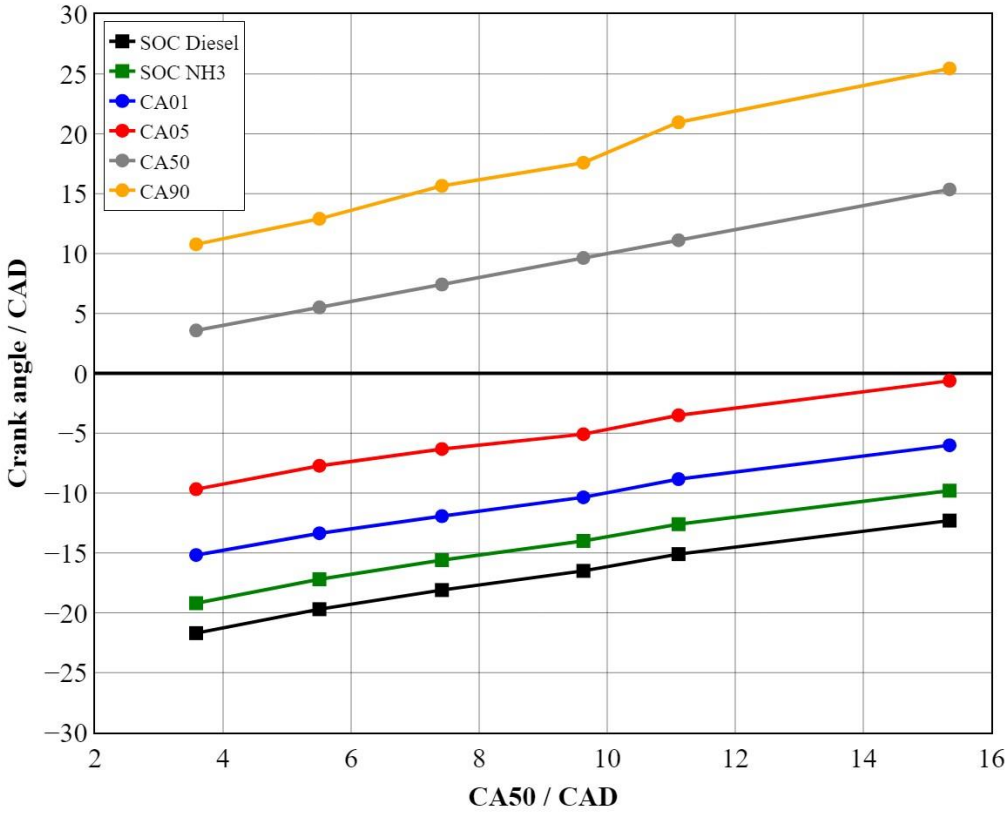

Figure 10: Injection timing and combustion progress for a combustion phasing variation at constant BMEP

A potential explanation for this unexpected trend can be seen in Figure 12 where the normalized heat release rates for the early combustion phase are shown. It can be observed that the time delay between the start of the diesel injection and the first rise of the heat release rate decreases with later injection timing, as expected due to the increasing pressures and temperatures later in the compression stroke. Again, due to the long hydraulic delay of the ammonia injector it is assumed that ammonia is not affecting this initial phase of the combustion. It can be observed, however, that with later injection timing the pre-mixed peak is reduced and the subsequent rapid increase of the heat release rate is retarded. It is hypothesized that two effects contribute to this behavior. On one hand, the shorter ignition delay time could reduce the spatial overlap of the ammonia and the diesel sprays and therefore the ignition of the ammonia spray. On the other hand, the reduced cylinder volume close to top dead center might impact the spray propagation and air entrainment.

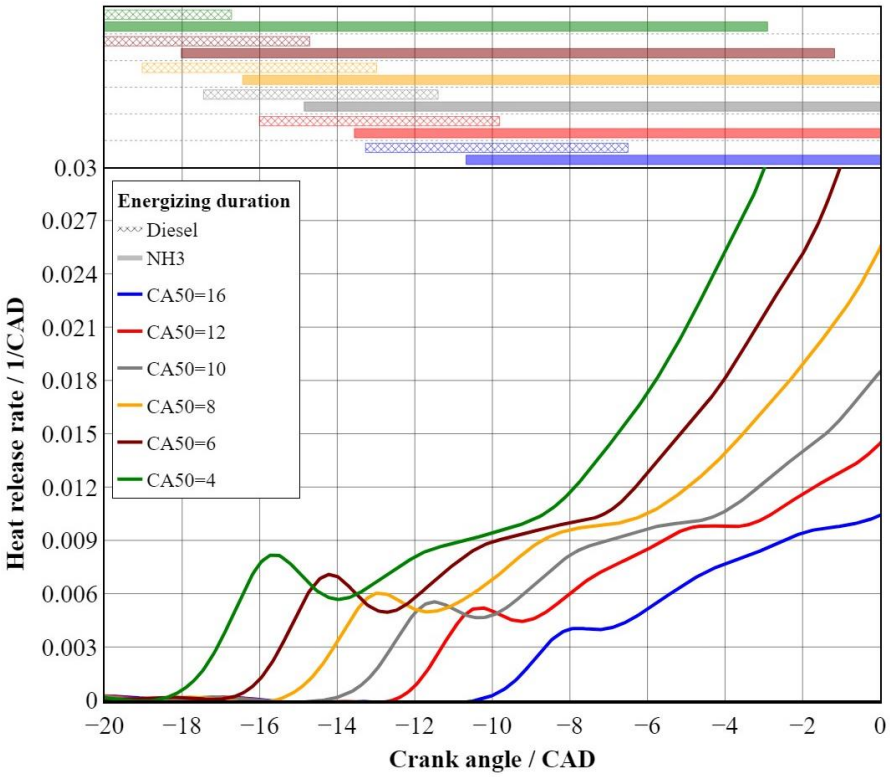

Figure 11: Heat release rate during ignition and early combustion phase for different combustion phasing

The impact of the slow increase in the heat release rate can be seen in the cumulative heat release in Figure 13. While the start of combustion shows a small spread only, the timing for CA50 shows a much higher spread from the earliest to the latest combustion phasing. This trend differs significantly from the behavior of a pure diesel combustion (with a centrally mounted diesel injector) that is shown in the bottom part of Figure 13. The cumulative heat release rates of the diesel combustion show less of a change in the shape but more a parallel shift of the curves. Apart from the interaction of the diesel and the ammonia sprays the fuel evaporation, especially the ammonia evaporation, could further impact the combustion process. Due to the significantly higher heat of vaporization the impact on combustion chamber temperature is expected to be significantly higher. The development of evaporation models and their integration into the heat release analysis tools is currently in progress and will allow a more detailed analysis of the ammonia combustion process in the future.

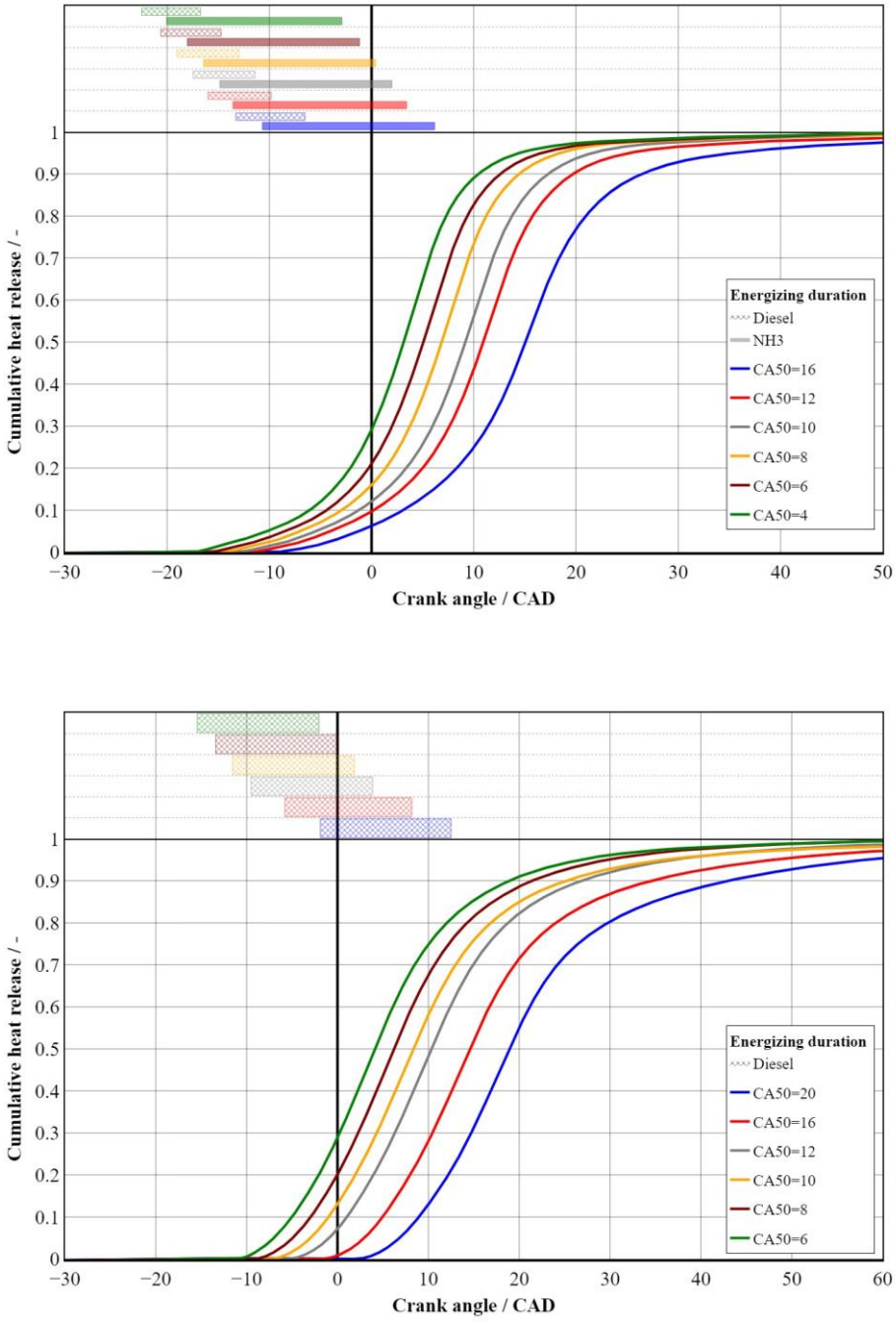

Figure 12: Cumulative heat release for different combustion phasing for ammonia (top) and diesel (bottom)

4.4. Comparison to diesel operation

The effect of the evaporative cooling can also explain some of the differences observed for a comparison of key parameters for ammonia and diesel combustion (Figure 14). The measured exhaust gas temperature for ammonia operation is approximately 100 K lower than for diesel operation with the same excess air ratio and combustion phasing. Reiter and Kong [18] performed thermodynamics calculations for the adiabatic flame temperature as a function of the fuel share between diesel and ammonia and the excess air ratio. They found that the adiabatic flame temperature for stoichiometric

conditions was reduced from 2320 K for diesel to 2100 K for ammonia and indicated the impact on the overall in-cylinder temperature level when ammonia is used as a fuel. The differences in the heat of vaporization between the fuels is exacerbating this effect. This impact on the in-cylinder temperature strongly affects the thermal NO_X formation that is typically the dominant share in hydrocarbon fuels. For ammonia combustion this temperature-driven effect is combined with the nitrogen oxide formation from fuel-bound nitrogen. The combined effect can be seen in the bottom of Figure 14 where the ammonia operation showed significantly lower nitrogen oxide emissions than the diesel combustion. The cyclic variability of the ammonia operation was higher than for diesel operation throughout the combustion phasing variation. Up to CA50 = 12 CAD aTDC the coefficient of variation of the indicated mean effective pressure (COV) could be maintained below 1.5%. For the latest combustion phasing of CA50 = 16 CAD aTDC the cyclic variability increased significantly which might be explained by the weak combustion initiation.

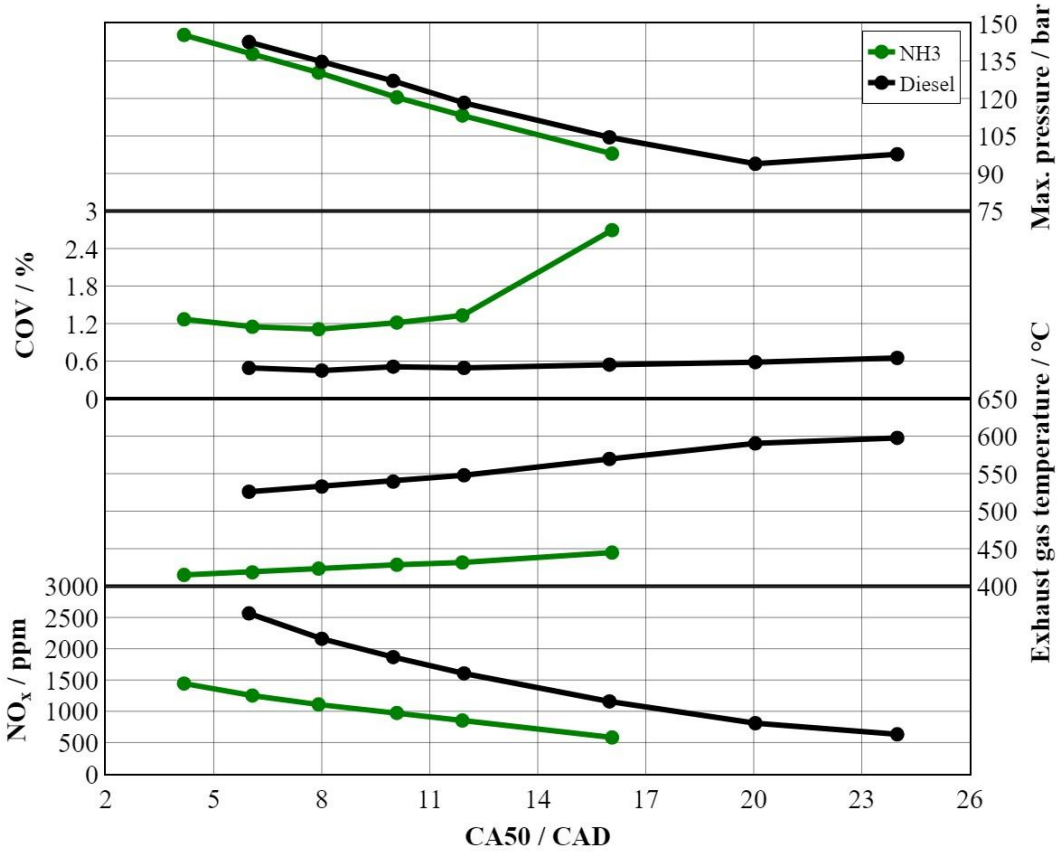

Figure 13: Selected performance parameter for the comparison of ammonia and diesel operation during a combustion phasing variation

Further analysis of the heat release rate of ammonia operation revealed that the cyclic variability is caused by the later part of the combustion. In Figure 15 the normalized heat release rates for a diesel operating point and an ammonia-diesel operating point with 10% diesel fraction are displayed. For both operating points the mean cycle (solid lines) as well as the standard deviation (shaded areas) are shown. For pure diesel operation the cyclic variability is very small and hardly visible in the diagram. For the ammonia combustion the early combustion phase has the same low cyclic variability that the diesel operation is showing. Only in the later part of the combustion where ammonia is burned the cyclic

variability increases significantly. Future work will have to determine the root cause and mitigation measures. At this point it is not entirely clear if some of the variability might originate from the fuel supply rather than the in-cylinder processes.

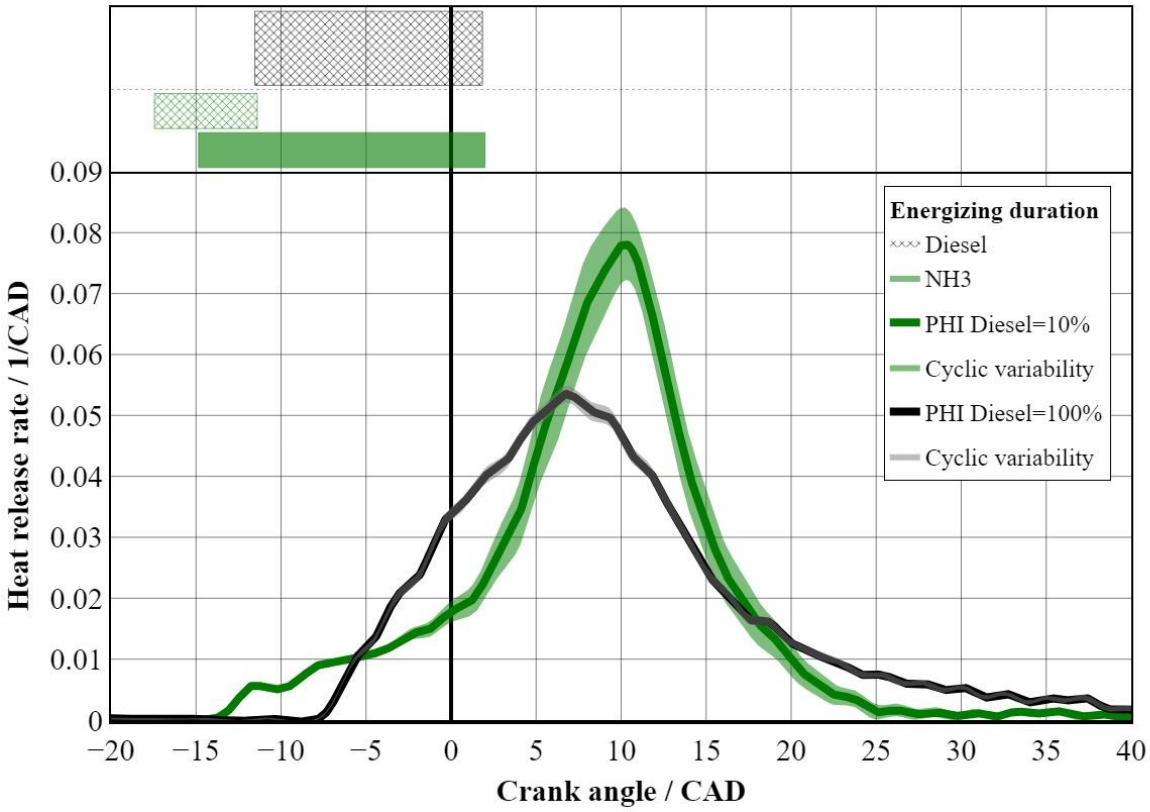

Figure 14: Illustration of cyclic variability of the heat release rate for ammonia and diesel operation

5. Conclusions

Ammonia is widely considered to be a strong candidate to serve an energy carrier for large-scale energy storage and transportation as the world transitions from a fossil fuel-based energy system to a system based on renewable energy. Although based on its physical and chemical properties ammonia does not seem to lend itself to direct use in internal combustion engines, recent progress has shown that ammonia is a suitable fuel for many applications. Different ammonia fuel admission and combustion concepts are currently under investigation to assess potential and limitations. In order to fulfill future stringent emission legislation exhaust gas aftertreatment will have to be an integral part of ammonia-based propulsion or power generation systems.

In this article an NH_3-HPDI combustion concept with a centrally mounted ammonia injector was experimentally evaluated on a medium-speed single cylinder research engine. Robust engine operation with ammonia energy shares up to 90% could be demonstrated and it was shown that moderate ammonia injection pressures of 60 MPa were sufficient to allow a wide operating range. Compared to previously published ammonia combustion investigations using port fuel injection or central mixture formation the use of high-pressure direct injection enabled a reduction of NH_3 emissions. NH_3 concentrations were mostly in the 1000 – 2000 ppm-range and for the best nozzle configuration concentrations of approximately 600 ppm were feasible even with excess air ratios typical for diesel

combustion concepts. The boost pressure demand does not increase compared to diesel operation such that existing turbocharger systems can potentially be modified to fulfill the needs of ammonia operation. The final excess air ratio selection will also have to take the exhaust gas temperature and its impact on the exhaust gas aftertreatment into account. In contrast to LNG dual fuel combustion concepts no combustion anomalies such as knocking have been observed for ammonia combustion, enabling the use of early combustion phasing. The benefits of the high excess air ratios and combustion phasing options support a favorable efficiency vs. NO_X trade-off that is illustrated in Figure 16. In comparison to the diesel operation a higher engine efficiency could be achieved with the NH_3-HPDI concept at a given NO_X intensity.

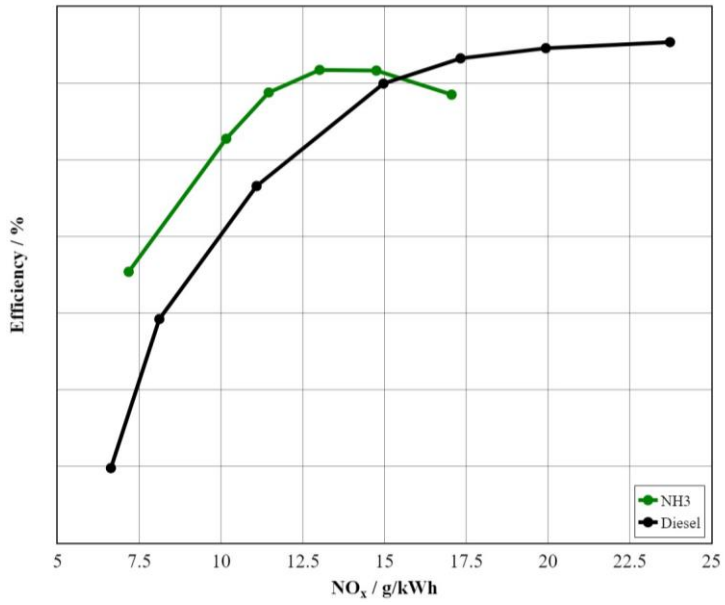

Figure 15: Efficiency vs. NO_X emission trade-off for ammonia and diesel operation

Future research on NH_3-HPDI combustion will focus on the optimization of the spray-spray and spray-piston bowl interaction as well as exhaust gas aftertreatment. Furthermore, the long-term impact of ammonia and ammonia combustion products on materials and lubricants will have to be subject to detailed investigations.

Literature

[1] Global Monitoring Laboratory, Trends in Atmospheric Carbon Dioxide, https://gml.noaa.gov/ccgg/trends/gl_gr.html, accessed: August 2023.

[2] Copernicus: 2023 is the hottest year on record, with global temperatures close to the 1.5°C limit, https://climate.copernicus.eu/copernicus-2023-hottest-year-record, accessed on April 6, 2024

[3] IPCC, 2022, Climate Change 2022: Mitigation of Climate Change. Contribution of Working Group III to the Sixth Assessment Report of the Intergovernmental Panel on Climate Change [P.R. Shukla, J. Skea, R. Slade, A. Al Khourdajie, R. van Diemen, D. McCollum, M. Pathak, S. Some, P. Vyas, R. Fradera, M. Belkacemi, A. Hasija, G. Lisboa, S. Luz, J. Malley, (eds.)].

Cambridge University Press, Cambridge, UK and New York, NY, USA. doi: 10.1017/9781009157926E.

[4] UNFCCC, Report of the Conference of the Parties on its twenty-first session, held in Paris from 30 November to 13 December 2015. Addendum. Part two: Action taken by the Conference of the Parties at its twenty-first session, https://unfccc.int/documents/909, accessed: August 2023.

[5] European Commission: "2030 Climate Target Plan". https://ec.europa.eu/clima/policies/eu-climate-action/2030_ctp_en#:~:text=With%20the%202030%20Climate%20Target,target%20of%20at%20least%2040%25, accessed on January 28th, 2021.

[6] European Commission: Recommendations for 2040 targets to reach climate neutrality by 2050, https://commission.europa.eu/news/recommendations-2040-targets-reach-climate-neutrality-2050-2024-02-06_en?prefLang=de, accessed on February 11, 2024.

[7] IMO: "Resolution MEPC.304(72) – Initial IMO Strategy on Reduction of GHG Emissions from Ships", https://wwwcdn.imo.org/localresources/en/KnowledgeCentre/IndexofIMOResolutions/MEPCDocuments/MEPC.304(72).pdf, accessed on December 29th, 2020.

[8] S. Laiminger, K. Payrhuber, N. Wermuth, A. Wimmer, The role of gas engines in a future energy market with sustainable fuels, presented at 30th CIMAC World Congress 2023: Meeting the Future of Combustion Engines, Busan, June, 2023.

[9] DNV Pathway to net zero emissions, 2023

[10] A. Valera-Medina, F. Amer-Hatem, A. K. Azad, I. C. Dedoussi, M. de Joannon, R. X. Fernandes, P. Glarborg, H. Hashemi, X. He, S. Mashruk, J. McGowan, C. Mounaim-Rouselle, A. Ortiz-Prado, A. Ortiz-Valera, I. Rossetti, B. Shu, M. Yehia, H. Xiao, M. Costa, Energy & Fuels, DOI: 10.1021/acs.energyfuels.0c03685.

[11] IPCC, The Earth's Energy Budget, Climate Feedbacks, and Climate Sensitivity. In Climate Change 2021: The Physical Science Basis. Contribution of Working Group I to the Sixth Assessment Report of the Intergovernmental Panel on Climate Change", https://www.ipcc.ch/report/ar6/wg1/, accessed: July, 2023.

[12] N. Wermuth, M. Malin, C. Schubert-Zallinger, M. Engelmayer, A. Wimmer, H. Schlick, T. Kammerdiener, Decarbonization of high-power systems: ammonia-hydrogen and ammonia-diesel combustion in HS engines (Paper No. 667), presented at 30th CIMAC World Congress 2023: Meeting the Future of Combustion Engines, Busan, June, 2023.

[13] N. Wermuth, C. Gumhold, A. Wimmer, M. Url, S. Laiminger, Energy Technology, DOI: /10.1002/ente.202301008

[14] M. Coppo, N. Wermuth, 2022. Powering a greener future: the OMT injector enables high-pressure direct injection of ammonia and methanol, pp. 68-81, Proceedings of the 7th RGMT, Rostock, Germany.

[15] M. Coppo et al., Detailed characterization and service experience of OMT injectors for dual-fuel medium- and low speed engines (Paper No. 267), presented at 29th CIMAC World Congress 2019, Vancouver, June, 2019.

[16] Westlye, F.R., Ivarsson, A. and Schramm. 2013. Experimental investigation of nitrogen-based emissions from an ammonia fueled SI engine, Fuel, 111: 239-247

[17] Miller, J.A., Glarborg, P. 1996. Modelling the Formation of N2O and NO2 in the Thermal De-NOx Process. In: Wolfrum, J., Volpp, HR., Rannacher, R., Warnatz, J. (eds) Gas Phase Chemical Reaction Systems. Springer Series in Chemical Physics, vol 61. Springer, Berlin, Heidelberg. https://doi.org/10.1007/978-3-642-80299-7_25

[18] Reiter, A.J., Kong, S.C. 2008. Demonstration of compression-ignition engine combustion using ammonia in reducing greenhouse gas emissions, Energy Fuels, 22, 5, 2963 – 2971